The Astrophysical Journal, 618:649–656, 2005 January 10

OBSCURATION OF ACTIVE GALACTIC NUCLEI BY CIRCUMNUCLEAR STARBURSTS

Yasuyuki Watabe and Masayuki Umemura
Center for Computational Sciences, University of Tsukuba, Ten-nodai, 1-1-1 Tsukuba,
Ibaraki 305-8577, Japan; watabe@ccs.tsukuba.ac.jp, umemura@ccs.tsukuba.ac.jp
Received 2004 June 8; accepted 2004 September 14

ABSTRACT

We examine the possibility of active galactic nucleus (AGN) obscuration by dusty gas clouds that spurt out from circumnuclear starburst regions. For this purpose, the dynamical evolution of gas clouds is pursued, including the effects of radiation forces by an AGN as well as a starburst. Here we solve the radiative transfer equations for clouds, taking into consideration the growth of clouds by inelastic cloud-cloud collisions and the resultant change in optical depth. As a result, if the starburst is more luminous than the AGN, gas clouds are distributed extensively above the galactic disk with the assistance of radiation pressure from the starburst. The total covering factor of gas clouds reaches a maximum of about 20%. After several 10^7 yr, gas clouds with larger optical depth form by cloud-cloud collisions; thereafter the clouds fall back as a result of weakened radiation pressure. The larger clouds undergo runaway growth and are eventually distributed around the equatorial plane on the inner sides of circumnuclear starburst regions. These clouds have an optical depth of several tens. The result is qualitatively consistent with the putative tendency that Seyfert 2 galaxies appear more frequently associated with starbursts than Seyfert 1 galaxies. On the other hand, if the AGN luminosity overwhelms that of the starburst, almost all clouds are ejected from the galaxy as a result of the radiation pressure from the AGN, resulting in the formation of a quasar-like object. The origin of obscuration of AGNs is discussed with relevant observations.

Subject headings: galaxies: active — galaxies: nuclei — galaxies: Seyfert — galaxies: starburst — quasars: general — radiative transfer

1. INTRODUCTION

The origin of active galactic nucleus (AGN) obscuration is a key issue for a thorough understanding of AGNs. In the context of the unified model, an obscuring torus has been thought to be responsible for the AGN obscuration, and the dichotomy of AGN types has been attributed to the viewing angle toward the AGN (see Antonucci 1993 for a review). However, recent observations on circumnuclear regions of AGNs have gradually revealed that Seyfert 2 galaxies appear to be more frequently associated with starbursts than Seyfert 1 galaxies (Heckman et al. 1989; Maiolino et al. 1997, 1998a; Perez-Olea & Colina 1996; Hunt et al. 1997; Malkan et al. 1998; Schmitt et al. 1999; Storchi-Bergmann et al. 2000; Gonzalez Delgado et al. 2001). Furthermore, quasars are mostly observed as type 1 AGNs, regardless of the star formation activity in host galaxies (Barvainis et al. 1992; Ohta et al. 1996; Omont et al. 1996; Schinnerer et al. 1998; Brotherton et al. 1999; Canalizo & Stockton 2000a, 2000b; Dietrich & Wilhelm-Erkens 2000; Solomon et al. 2003). In addition, Ueda et al. (2003) have recently found from the hard X-ray luminosity function of AGNs that the fraction of X-ray–absorbed AGNs decreases with the AGN luminosity. These recent findings seem beyond comprehension in the context of the unified model.

The frequent association of circumnuclear starbursts with Seyfert 2 galaxies suggests that the obscuring of AGNs could be physically related to starburst events. Ohsuga & Umemura (1999, 2001) have considered a physical mechanism to link the AGN type to the circumnuclear starburst, where an obscuring wall composed of dusty gas can form with the assistance of radiation pressure from circumnuclear starbursts. More recently, Wada & Norman (2002) have performed three-dimensional hydrodynamic simulations on the nuclear starburst regions and found that the gas blown out from a galactic disk due to multiple supernova (SN) explosions in a starburst builds up a torus-like structure in a highly inhomogeneous and turbulent manner. Both models may provide potential mechanisms to relate the starburst events with the obscuring of AGNs. But Ohsuga & Umemura focused solely on the equilibrium configuration of dusty gas, while Wada & Norman did not include radiation forces, which are likely to play an important role in the early phase of starbursts. Hence, in order to construct a more realistic model, the dynamical evolution of obscuring materials should be solved, including radiation forces. This requires a radiation-hydrodynamic (RHD) simulation in three-dimensional space. However, a full RHD simulation is extremely time-consuming, even using state-of-the-art computational facilities. In this paper we solve the dynamics of discrete clouds under the adhesion approximation, where the growth of clouds is brought by inelastic cloud-cloud collisions. Simultaneously, to properly include the radiation forces, we solve the radiation transfer equation for clouds, taking the change in optical depth due to the cloud growth into account. In § 2 the circumnuclear regions and gas clouds are modeled. In § 3 we formulate the equation of motion for gas clouds including radiation forces. In § 4 the numerical results are shown, and the distribution of gas clouds and the obscuration of AGN are analyzed. In § 5 on the basis of these results, we discuss the origin of AGN obscuration and the relation to narrow-line regions (NLRs). Section 6 is devoted to the conclusions.

2. MODEL

Recent high-resolution observations have revealed circumnuclear starburst regions with a radial extension of 10 pc up to 1 kpc that frequently exhibit a ringlike feature (Pogge 1989; Wilson et al. 1991; Forbes et al. 1994; Marconi et al. 1994; Mauder et al. 1994; Buta et al. 1995; Barth et al. 1995; Leitherer

et al. 1996; Maoz et al. 1996; Storchi-Bergmann et al. 1996; Elmouttie et al. 1998). In this paper, we suppose a starburst region in ring configuration with a radius of 200 pc; the total mass of starburst ring is assumed to be $M_{\rm SB} = 10^8\ M_\odot$, similar to the model by Ohsuga & Umemura (2001). Also, we choose a galactic bulge component with mass of $M_{\rm GB} = 10^{10}\ M_\odot$ and radius of $R_{\rm GB} = 1$ kpc.

In some galaxies, a galactic bulge cannot solely explain the observed rotation curve. For instance, in the circumnuclear regions of the Circinus galaxy, the rotation velocity requires an additional component with 10^9–$10^{10}\ M_\odot$ within a starburst ring (Elmouttie et al. 1998). Also, the stellar velocity dispersion suggests that the Circinus galaxy has a spread component within a radius of several 100 pc (Maiolino et al. 1998a). In this paper, taking such mass distributions into consideration, we also assume an inner bulge component with mass of $M_{\rm IB} = 10^9\ M_\odot$ and radius of $R_{\rm IB} = 100$ pc. As for a central supermassive black hole (SMBH), the mass is assessed in terms of the recently inferred black hole–to–bulge mass relation, that is, $M_{\rm BH}/M_{\rm bulge} \approx 10^{-3}$ (Richstone et al. 1998, Marconi & Hunt 2003, and references therein). Here the SMBH mass is set at $M_{\rm BH} = 10^7\ M_\odot$.

We assume the energy spectrum of AGNs to be between 0.01 and 100 keV in the form $L^\nu_{\rm AGN} \propto \nu^{-1}$ (Blandford et al. 1990). The bolometric luminosity, $L_{\rm AGN}$, is set to be constant for a period of 10^8 yr, which is a typical age for AGNs (basically the Eddington timescale). In the starburst regions, we assume a Salpeter-type stellar initial mass function (IMF) for a mass range of $[m_l,\ m_u]$,

$$\phi(m_*) = \phi_0 (m_*/M_\odot)^{-(1+s)}, \tag{1}$$

where $s = 1.35$ and m_* is the stellar mass. Although m_l and m_u in starburst regions are under debate, some authors argue that the IMF in a starburst is deficient in low-mass stars, where $m_l \approx 2\ M_\odot$ is derived. The upper limit is inferred to be $m_u \approx 40\ M_\odot$ (Doyon et al. 1992; Charlot et al. 1993; Doane & Mathews 1993; Hill et al. 1994; Blandle et al. 1996). We assume these values for m_l and m_u. The star formation rate, $\dot{M}_*$, is controlled by $\dot{M}_* = (M_{\rm SB}/t_{\rm SF}) \exp(-t/t_{\rm SF})$, where t is the elapsed time after the initial starburst and $t_{\rm SF}$ is the duration of star formation, which is assumed to be 10^7 yr (e.g., Efstathiou et al. 2000). We employ a stellar mass–to-luminosity relation as $(l_*/L_\odot) = (m_*/M_\odot)^q$ with $q = 3.7$, and a stellar mass–to-age relation as $t_* = 1.1\times10^{10}\ {\rm yr}(m_*/M_\odot)^\omega$ with $\omega = 2.7$ (Lang 1974). All stars are assumed to emit the radiation in the blackbody.

Next we model the mass ejection from the starburst regions. The mass ejection is driven by multiple SN explosions in a starburst. Stars heavier than $m_{\rm crit} = 8\ M_\odot$ are destined to undergo Type II SN explosions. The SNe restore almost all the mass into interstellar space and release the energy with a conversion efficiency to the rest mass energy as $\epsilon \approx 10^{-4}$. Thus, the rate of mass restoration by SNe is assessed by $\dot{M}_{\rm SN}(t) = L_{\rm SN}(t)/c^2\epsilon$, where $M_{\rm SN}(t)$ is the total mass of SNe that explode by time t and $L_{\rm SN}(t)$ is the total SN luminosity that is temporally averaged. The energy input by multiple SN explosions leads to the formation of an elongated hot cavity (*superbubble*), and consequently the shock-heated interstellar gas spurts out from the starburst regions (Shapiro & Field 1976; Tomisaka & Ikeuchi 1986; Norman & Ikeuchi 1989). A recent simulation by Wada & Norman (2002) has shown that the shock-heated gas eventually fragments into cold, dense gas clouds because of the cooling. Hence, we simply suppose that gas clouds spurt from the starburst regions with the mass restoration rate estimated above. (We note that a portion of the preexisting interstellar gas could be also accelerated by the superbubble and therefore participate in the mass ejection from a starburst. Hence, the present mass ejection rate is regarded as a minimum rate.) On the basis of the Wada & Norman results, we set the initial cloud radius and mass to be $r_c = 3.5$ pc and $M_c = 10^3\ M_\odot$ as a fiducial model. Then the hydrogen density in a cloud is $2\times10^2\ {\rm cm}^{-3}$. We also examine the effect of a different initial size of clouds by setting $r_c = 2.5$ or 4.5 pc. The cloud velocity is assumed to be $V_c \sim 150\ {\rm km\ s}^{-1}$, which is on the order of escape velocity. Figure 1 shows the evolution of mass ejection rate (*solid line*) and luminosity (*dashed line*) in the starburst regions. Before 4.3×10^7 yr, the starburst is super–Eddington-luminous for gas clouds of initial size. As for the effects of photoionization and photodissociation by the radiation from a starburst as well as an AGN, Ohsuga & Umemura (2001) have analyzed the inner structure of an optically thick gas slab by solving the force balance and the energy equation. They found that the dust cooling is still effective for a gas slab located at several hundred parsecs from the galactic center, and the resultant gas temperature is on the order of 100 K. Hence, we assume the cloud temperature to be 100 K and the optical depths of clouds to be determined by the dust opacity.

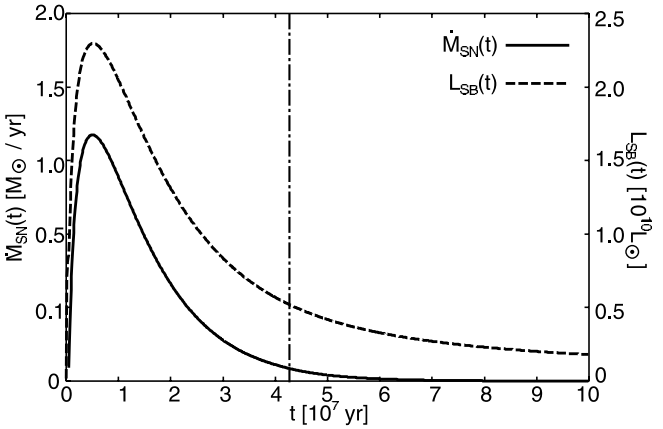

FIG. 1.—Evolution of the mass ejection rate (*solid line*) and luminosity of the starburst region (*dashed line*). The starburst is super–Eddington-luminous for gas clouds of initial size before the epoch $\sim4.3\times10^7$ yr (*dot-dashed line*).

The spurted clouds can collide with each other in the space above the galactic disk. Here we simply assume that an inelastic collision occurs if the distance between cloud centers is less than the sum of cloud radii. Also, it is assumed that the density of clouds does not alter after the collision, so that a cloud of larger size is generated by the collision. Taking into account the resultant change in optical depth of clouds, we calculate the dilution of the radiation from a starburst and an AGN. It should be noted that this assumption on the collision is quite naive. Nagasawa & Miyama (1987) have simulated the head-on collisions of isothermal clouds, using a three-dimensional hydrodynamic code, and have found that the cloud-cloud collisions are very inelastic even for a Mach number of 10 and result in the coalescence without disruption. However, in our simulation, the Mach number can be up to several tens or $\sim$100. Also, the off-center collisions can frequently occur. In this case, the cloud-cloud collision may result in not only the coalescence but also the disruption of clouds or the induction of star formation. These effects seem worth incorporating in the future simulations.

The self-gravity of clouds is $\sim 10^{-3}$ of the external gravity in the model galaxy. Hence, the self-gravity of clouds can be neglected. But the growth of clouds induced by collisions can lead to the gravitational instability if the cloud radii exceed the Jeans scale, which is 10.8 pc for the assumed cloud temperature of 100 K. In this simulation, we treat a cloud above the Jeans scale as a collapsing cloud that no longer contributes to the obscuration.

3. BASIC EQUATIONS

The equation of motion is given by

$$\frac{d^2\boldsymbol{r}}{dt^2} = \boldsymbol{f}_{\mathrm{rad,SB}} + \boldsymbol{f}_{\mathrm{rad,AGN}} + \boldsymbol{f}_{\mathrm{grav,SB}} + \boldsymbol{f}_{\mathrm{grav,BH}} + \boldsymbol{f}_{\mathrm{grav,bulge}}, \quad (2)$$

where $\boldsymbol{r}$ is the position vector of a cloud from the galactic center, and $\boldsymbol{f}_{\mathrm{grav,SB}}$, $\boldsymbol{f}_{\mathrm{grav,BH}}$, and $\boldsymbol{f}_{\mathrm{grav,bulge}}$ are the gravitational forces from the starburst ring, the central SMBH, and the bulges, respectively. The radiation pressure force from the starburst, $\boldsymbol{f}_{\mathrm{rad,SB}}$, is given by

$$\boldsymbol{f}_{\mathrm{rad,SB}} = \int_V dV \frac{\bar{\chi}_{\mathrm{SB}}}{c} \frac{\rho_{\mathrm{SB}}(t)}{4\pi|\vec{\boldsymbol{l}}_{\mathrm{SB}}|^3} \boldsymbol{l}_{\mathrm{SB}} \left[\frac{1 - \exp(-\tau_{\mathrm{SB}})}{\tau_{\mathrm{SB}}}\right], \quad (3)$$

where $\bar{\chi}_{\mathrm{SB}}$ is the mass extinction coefficient, which is averaged over the spectrum of the starburst and $\bar{\chi}_{\mathrm{SB}} = \int_\nu \chi_\nu L^\nu_{\mathrm{SB}} d\nu / L_{\mathrm{SB}}$, where χ_ν is the mass extinction coefficient and L^ν_{SB} is the spectrum. Since the mass density is dominated by gas with little contribution of dust and the Thomson scattering is negligible in the opacity (Umemura et al. 1997, 1998), χ_ν is given by $\chi_\nu = \kappa^d_\nu / \rho_g$, where κ^d_ν is the opacity by dust grains per unit volume and ρ_g is the gas density in a cloud. Here τ_{SB} is the cloud optical depth estimated by $\bar{\chi}_{\mathrm{SB}}$, $\rho_{\mathrm{SB}}(t)$ is the luminosity density in the starburst region, and $\boldsymbol{l}_{\mathrm{SB}}$ is the position vector of a cloud from a volume element dV in the starburst region. We suppose the dust-to-gas mass ratio to be 0.03, which is 3 times as high as that observed in the solar neighborhood, because the metallicity in QSOs is found to be several to 10 times higher than the solar metallicity (e.g., Hamann & Ferland 1993). Here we employ a grain size distribution of a power law as $n_d(a_d) \propto a_d^{-3.5}$ in the range of 0.01–1 μm, which is found in the interstellar matter (Mathis et al. 1977); the absorption cross section is determined by $\pi a_d^2 \min[1, (2\pi\nu a_d/c)^2]$, where a_d is the grain radius. The density of solid material within a grain is assumed to be 1.0 g cm^{-3} (e.g., Spitzer 1978). We find the resultant optical depth of a gas cloud to be $\tau_c \sim 4$.

Similar to the starburst case, the radiation pressure force from the AGN, $\boldsymbol{f}_{\mathrm{rad,AGN}}$, is calculated by

$$\boldsymbol{f}_{\mathrm{rad,AGN}} = \frac{\bar{\chi}_{\mathrm{AGN}}}{c} \frac{L_{\mathrm{AGN}}}{4\pi|\boldsymbol{r}|^3} \boldsymbol{r} \left[\frac{1 - \exp(-\tau_{\mathrm{AGN}})}{\tau_{\mathrm{AGN}}}\right], \quad (4)$$

where $\bar{\chi}_{\mathrm{AGN}}$ is the mass extinction coefficient, which is averaged over the spectrum of the AGN, and τ_{AGN} is the optical depth estimated by $\bar{\chi}_{\mathrm{AGN}}$. Here we neglect the radiation force from SNe, because the average luminosity of SNe in the assumed IMF is less than 10% of the total stellar luminosity of starbursts.

4. NUMERICAL RESULTS

Here we show the numerical results for a starburst-dominant case and an AGN-dominant case. In each case, the time variations of the spatial distributions of gas clouds are presented, and the obscuration of AGNs by the clouds is analyzed.

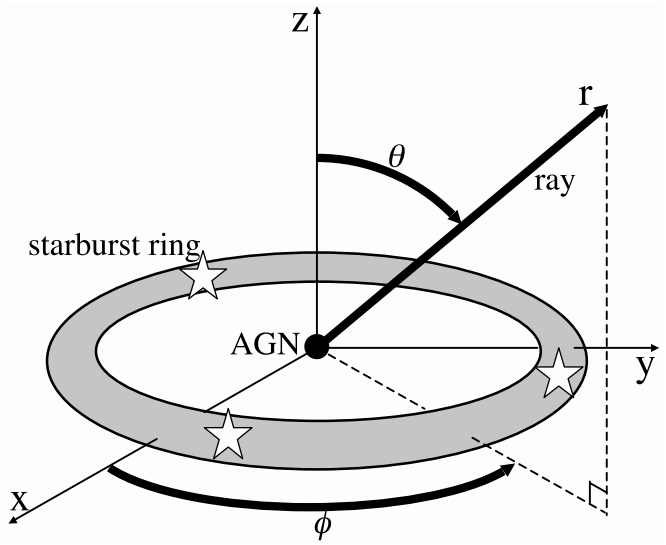

FIG. 2.—Schematic view of the circumnuclear structure and the coordinate system.

4.1. *Starburst-dominant Case*

We consider a case with $L_{\mathrm{AGN}} = 10^{10}\, L_\odot$. The AGN luminosity is lower than the starburst luminosity until $\sim 3 \times 10^7$ yr. To show the cloud distributions, we use the coordinates depicted in Figure 2. The resultant cloud distributions projected onto the *rz*- and the *xy*-plane are shown in the left panels of Figure 3. The colors of points stand for the cloud radii, where blue points are 3.5 pc, which corresponds to the clouds missing collisions, and red ones are the maximum radius of 10.8 pc, which is the Jeans radius. Using the resultant cloud distributions, we calculate the optical depth, τ, toward the direction with θ and ϕ. Taking the impact parameter into account, τ is given by

$$\tau = \sum_{i, b(i) \le r_c(i)} 2 \left[1 - \frac{b(i)^2}{r_c(i)^2}\right]^{1/2} \tau_c(i), \quad (5)$$

where i denotes each gas cloud, $b(i)$ is the impact parameter (the distance from the cloud center to the line of sight), $\tau_c(i)$ is the optical depth of the cloud along the diameter, and $r_c(i)$ is the cloud radius. If $b(i) \le r_c(i)$, the clouds contribute to the optical depth. The right panels in Figure 3 show τ for each direction of (θ, ϕ), using the Mollweide projection for the all-sky plot. The colors represent the levels of τ, ranging from 0 (*white*) to 50 (*red*).

As shown in Figure 3, gas clouds are distributed extensively above the starburst ring at the stage of $\sim 10^7$ yr. The radiation pressure from the starburst works to accelerate clouds, because the starburst is super–Eddington-luminous until 4.3×10^7 yr for gas clouds of initial size. But clouds are not distributed around the polar regions. This is because clouds are ejected from the rotating starburst ring and thus possess angular momenta. At this stage, the formation of larger clouds by cloud-cloud collisions is not promoted to a great extent. At $\sim 2 \times 10^7$ yr, clouds with large optical depths increase by repetitive cloud-cloud collisions, and they fall back as a result of the reduced radiation pressure per unit mass. The larger clouds undergo runaway growth and are eventually distributed around the equatorial

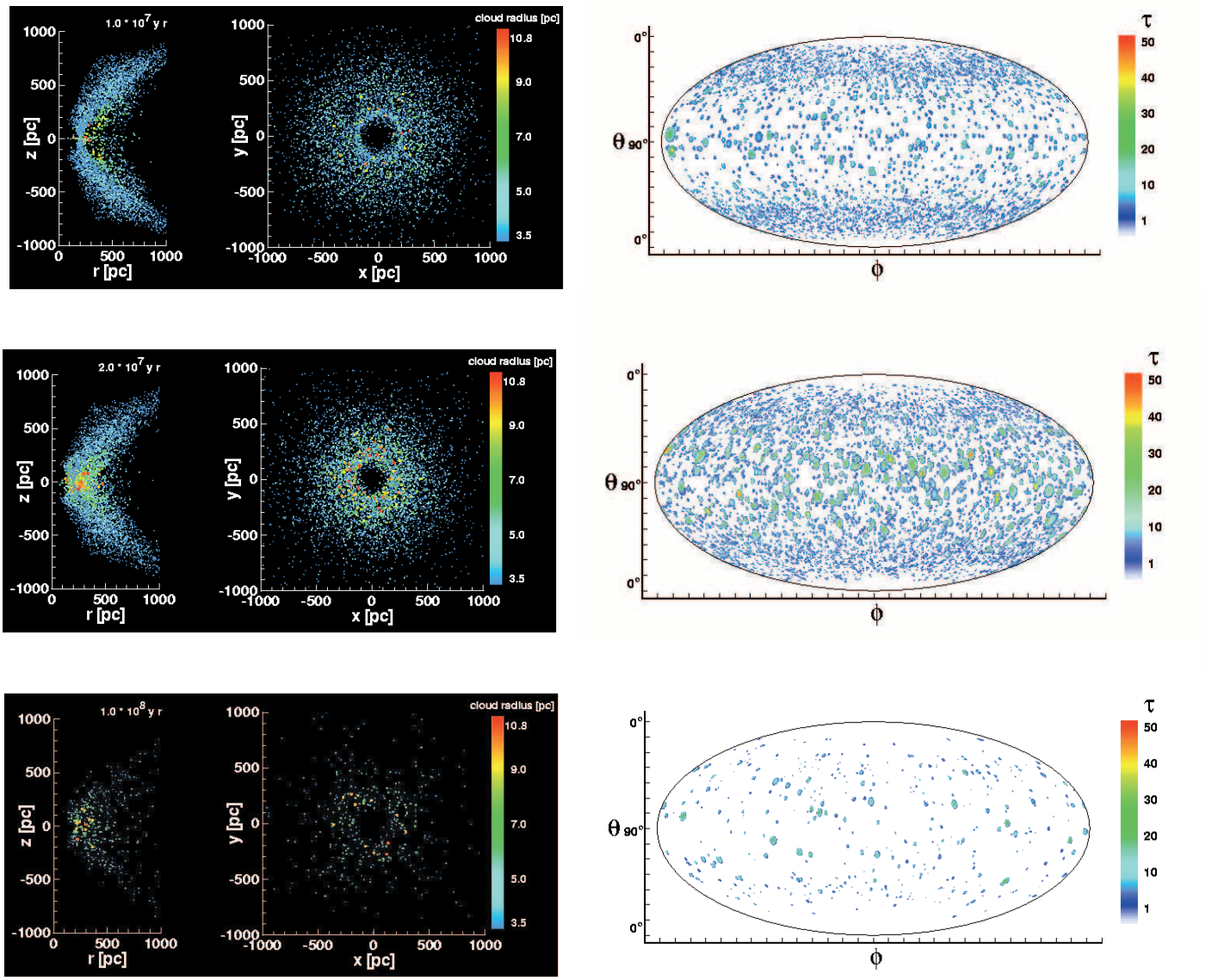

FIG. 3.—Distributions of gas clouds and optical depth to AGNs; $L_{\rm AGN} = 10^{10}\ L_{\odot}$ is assumed. We show snapshots at 10^7, 2×10^7, and 10^8 yr. The left panels display the cloud distributions projected on the *xy*- and the *rz*-plane in the coordinates shown in Fig. 2. The colors of the points correspond to the radii of gas clouds. The right panels show τ for the each direction $(\theta,\ \phi)$ using the Mollweide projection for the all-sky plot. The colors of the points correspond to the levels of τ.

plane on the inner sides of circumnuclear starburst regions. These clouds have an optical depth of several tens. The angular momentum transfer by cloud collisions near the equatorial plane is not so efficient to allow effective mass accretion on to the AGN. Therefore, the large clouds stay there and can contribute to the obscuration of the AGN. At $\sim10^8$ yr, the starburst luminosity becomes sub-Eddington for all clouds, and therefore gas clouds fall back one after another. At this stage, a large quantity of clouds exceed the Jeans size, and thus the number of obscuring clouds decreases rapidly. In Figure 4 the transition of the mass spectrum of the clouds is shown. This figure demonstrates the collision-induced growth of clouds and the decrease of obscuring clouds by the Jeans instability.

Next we evaluate the covering factor of obscuring clouds. Figure 5 shows the time variations of the covering factor, which is defined by the fraction of the area in the sky with the optical depth (τ) larger than the optical depth given in the abscissa. If we see the covering factor of $\tau > 2-3$, it changes from $\sim$13% at 10^7 yr to a maximum of $\sim$21% at 2×10^7 yr. This result shows that the starburst-origin dusty clouds can contribute to the obscuration of AGNs to a notable extent. After that, the covering factor lessens because of the fallback of clouds.

To see the effect of a different choice of initial size of gas cloud, we also calculate models with an initial cloud radius of $r_c = 2.5$ or 4.5 pc without changing the cloud mass. In Figure 6 we show the resultant covering factor against the optical depth. If the spatial distribution is the same, the shrink of clouds would result in the reduction of the covering factor as a result of the smaller geometrical cross section of clouds. The reduction of covering factor would be a factor of $(2.5/3.5)^2 = 0.51$, if $r_c = 2.5$ pc is assumed. But, as seen in Figure 6, the actual reduction of peak covering factor is $0.16/0.21 = 0.76$. This can be understood by the effect of radiation pressure. If the initial cloud size is smaller, the optical depth of a cloud becomes larger. Hence, the radiation pressure on a cloud is weakened, so that clouds are distributed in a more compact space. This effect tends to enlarge the covering factor. On the other hand, for the case of $r_c = 4.5$ pc, the peak covering factor increases by just a small factor of $0.23/0.21 = 1.1$, although the geometrical cross section would lead to an increase of covering factor by

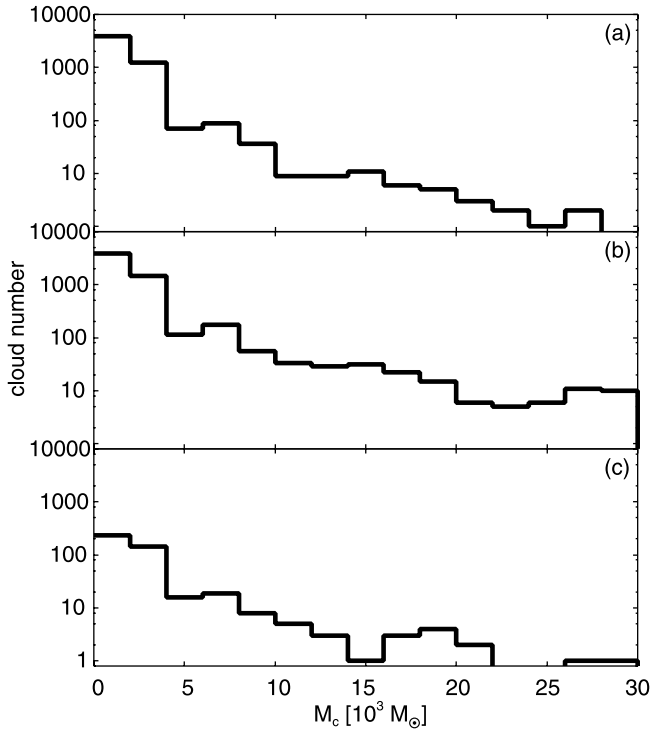

FIG. 4.—Mass spectrum of clouds at (*a*) 10^7, (*b*) 2×10^7, and (*c*) 10^8 yr. The horizontal axis represents the cloud mass in units of $10^3\ M_\odot$, while the vertical axis represents the cloud number.

$(4.5/3.5)^2 = 1.65$. There is again the radiation pressure effect. Expanded clouds can be distributed more sparsely by less diluted radiation pressure, so that the covering factor is reduced. In addition, larger clouds more frequently collide with each other. This effect also reduces the covering factor. As a result, it turns out that the peak covering factor is not so sensitive to the initial size of clouds.

4.2. *AGN-dominant Case*

Here we show the results of an AGN-dominant case, where $L_{\rm AGN} = 3\times10^{11}\ L_\odot$ is assumed. In this case, the AGN luminosity is higher than the starburst luminosity all the time. Figures 7 and 8 show the results by the same quantities as Figures 3 and 5, respectively. The assumed AGN luminosity

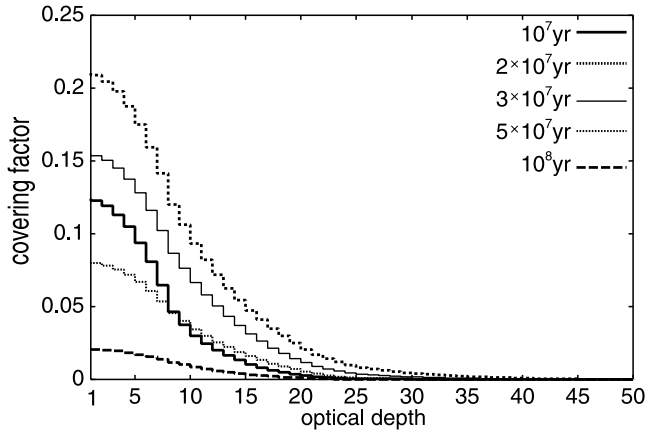

FIG. 5.—Covering factor of the area whose line-of-sight optical depth is greater than an optical depth given in the horizontal axis; $L_{\rm AGN} = 10^{10}\ L_\odot$ is assumed. The evolution of the covering factor is shown at 1, 2, 3, 5, and 10×10^7 yr.

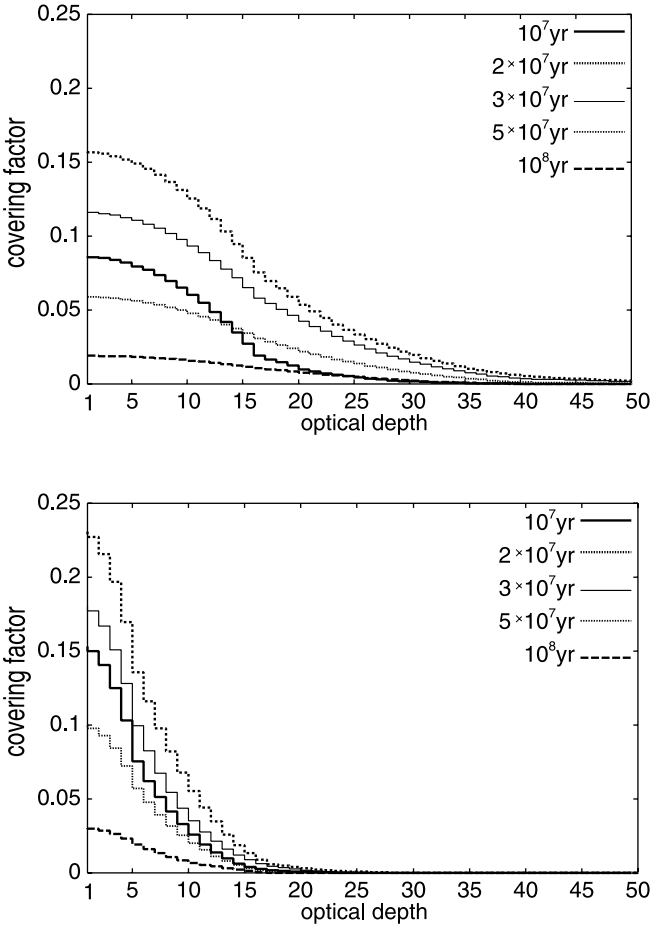

FIG. 6.—Same as Fig. 5, but the initial cloud radius is 2.25 pc (*top*) and 4.5 pc (*bottom*).

is close to the Eddington luminosity for the total mass of the galaxy. Hence, gas clouds are vigorously accelerated. Even at the early stage of $\sim10^7$ yr, clouds are already distributed over kiloparsecs, as shown in Figure 7. Very few collisions occur because the radiation pressure from the AGN drives a spreading outflow of clouds. At $\sim2\times10^7$ yr, a large fraction of clouds escape from the galaxy, so that most gas clouds cannot contribute to the obscuration of AGNs. At $\sim10^8$ yr, a small number of collision-induced large clouds are left.

Because of the cloud motion driven by the AGN luminosity, the covering factor of obscuring clouds cannot reach a higher level. The maximum covering factor is $\sim$5% at 10^7 yr, as shown in Figure 8. Hence, the AGN is likely to be observed as a type 1 with high probability. Such an AGN-dominant case may correspond to quasar events. The relation between AGN type and luminosity is discussed below in the context of the obscuration.

5. DISCUSSION

5.1. *Origin of Obscuration*

In the previous section, it was shown that the covering factor of starburst-origin dusty clouds increases during the luminous phase of the circumnuclear starburst. This can provide a qualitative explanation for the fact that Seyfert 2 galaxies are more frequently associated with starbursts than Seyfert 1 galaxies. On the other hand, obscuring clouds are not distributed around polar regions, as shown in Figure 3. Thus, in the face-on view, the AGN is likely to be identified as a type 1 even in a luminous phase of starburst, if there is no obscuring materials other than

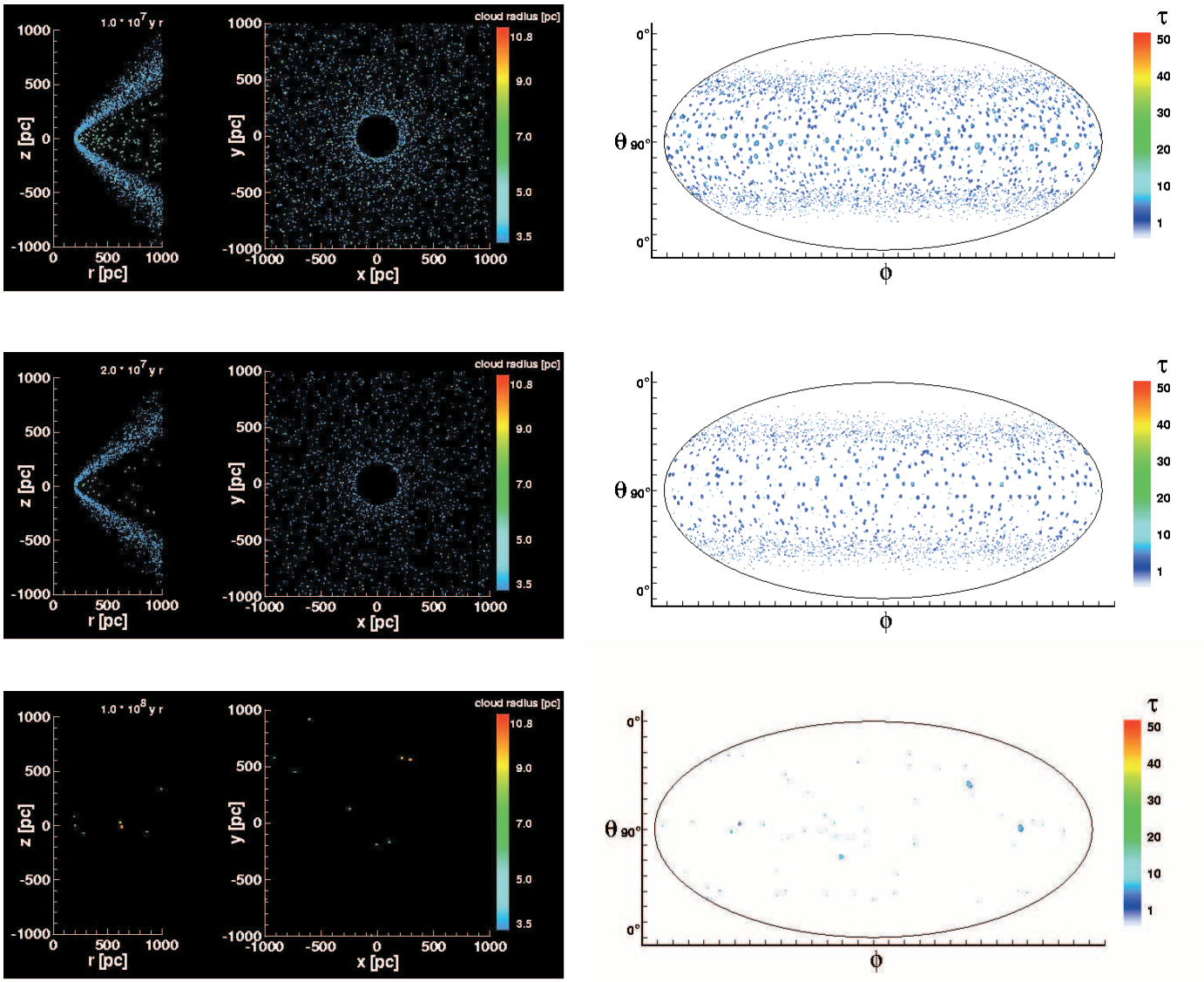

FIG. 7.—Same as Fig. 3, but $L_{\rm AGN} = 3\times10^{11}\ L_{\odot}$ is assumed. In this case, since the radiation pressure from the AGN is high, most of the gas clouds cannot contribute to the obscuration of the AGN.

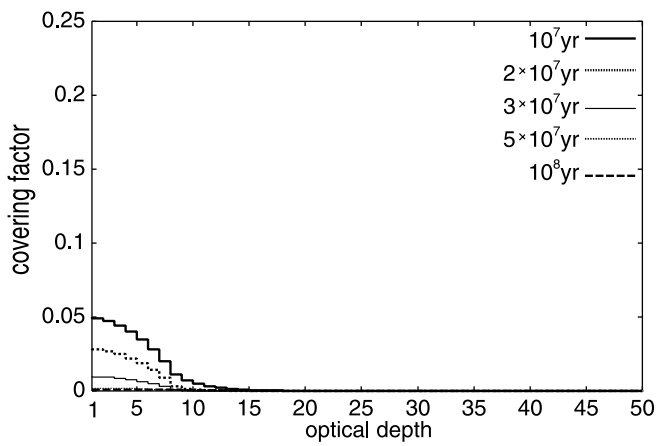

FIG. 8.—Same as Fig. 5, but for $L_{\rm AGN} = 3\times10^{11}\ L_{\odot}$.

starburst-origin dusty clouds. In that sense, Seyfert 1 galaxies may be coupled with starburst events. Interestingly, hidden starbursts have been found in Seyfert 1 galaxies (Imanishi & Dudley 2000; Rodríguez-Ardila & Viegas 2003), and there is also an example of Seyfert 1 galaxies accompanied by circumnuclear starbursts, namely, NGC 7469 (Genzel et al. 1995).

In this simulation, if we see the starburst ring at face-on view, starburst-origin dusty clouds obscure 30% of the starburst ring at maximum. This covering factor is not sufficient to produce perfectly hidden starbursts. However, further effects can change the covering factor. In the present simulation, we have ignored collapsing clouds above the Jeans scale. But the collapsing clouds are likely to result in the star formation. Hence, the re-ejection of matter by SNe in the collapsed object may also contribute to the obscuring. Furthermore, in light of the tight correlation between SMBHs and galactic bulges (Richstone et al. 1998; Marconi & Hunt 2003; Kawakatu & Umemura 2004), a starburst in a bulge may contribute to the obscuration of nuclear regions (e.g., Umemura 2001; Kawakatu et al. 2003).

As for the ratio of Seyfert 2 to 1 galaxies, Maiolino & Rieke (1995) concluded that Seyfert 2 galaxies appear to be 4 times more numerous than Seyfert 1 galaxies. This implies that the total covering factor of obscuring materials is likely to be of order 80%. In this simulation, the maximum covering factor is around 20%. A hydrodynamic simulation by Wada & Norman (2002) also shows the covering factor to be 40% at an early phase (1.6 Myr) of starburst. Hence, it seems that additional obscuring materials are required to account for the number ratio between Seyfert 1 and Seyfert 2 galaxies. Recently, we have some significant pieces of observational information about the obscuring materials. The A_V of the nuclear or circumnuclear regions is estimated to be between a few and several magnitudes by IR and optical observations (Rix et al. 1990; Roche et al. 1991; Goodrich et al. 1994; McLeod & Rieke 1995; Oliva et al. 1999). On the other hand, X-ray observations have shown that most Seyfert 2 nuclei are heavily obscured along the line of sight with at least $A_V > 10$ mag and sometimes $A_V > 100$ mag (Matt et al. 1996, 1999; Maiolino et al. 1998b; Bassani et al. 1999; Risaliti et al. 1999). Also, it is argued that a component of obscuring materials must be extended up to $\geq$100 pc in addition to a compact component confined to subparsec scales (Rudy et al. 1988; Miller et al. 1991; Goodrich 1995; McLeod & Rieke 1995; Maiolino et al. 1995; Maiolino & Rieke 1995; Malkan et al. 1998). These findings suggest that the distributions of dusty gas around an AGN are much more diverse than previously considered. The dusty clouds ejected from starbursts may be the origin of the extended obscuring matter. In addition, inner obscuring materials (possibly a dusty torus) may cooperatively work to obscure the nucleus. The combination of outer and inner obscuring materials will be an important issue to be scrutinized.

For the case in which the AGN luminosity is predominant, dusty clouds are blown out from a galaxy by the AGN radiation pressure and therefore cannot contribute much to the obscuration. This result matches the fact that quasars are mostly observed as type 1 AGNs, regardless of the star formation activity in host galaxies (Barvainis et al. 1992; Ohta et al. 1996; Omont et al. 1996; Schinnerer et al. 1998; Brotherton et al. 1999; Canalizo & Stockton 2000a, 2000b; Dietrich & Wilhelm-Erkens 2000; Solomon et al. 2003). Also, on the basis of the hard X-ray luminosity function of AGNs, Ueda et al. (2003) have found that the fraction of X-ray–absorbed AGNs decreases with the AGN luminosity. This trend is also consistent with the present picture of the radiation pressure-induced outflow.

5.2. *Relation to NLRs*

It is intriguing to consider the possible relation between dusty clouds and NLRs in AGNs, because the velocity dispersion of starburst-origin clouds, a few 100 km s^{-1}, is just on the order of that found in NLRs. One of the common properties of NLRs is a fairly constant ionization parameter, i.e., $U \equiv S/nc \approx 0.01$, where S is the ionizing photon flux and n is the density at irradiated cloud surfaces. Recently, Dopita et al. (2002) argued that the ionization parameter of NLRs is successfully accounted for by radiation pressure-dominated dusty photoablating clouds. This picture seems quite consistent with the present model. In addition, it is reported that Seyfert 1 galaxies have a smaller number of narrow-line clouds than Seyfert 2 galaxies (Schmitt 1998), and also the extension of NLRs in AGNs is roughly proportional to the square root of the [O III] luminosity (Bennert et al. 2002). These trends are qualitatively compatible with the present results that the number of dusty clouds decreases with a dimming starburst, and the spatial extent of dusty clouds augments with increasing AGN luminosity.

6. CONCLUSIONS

We have investigated the dynamics of gas clouds that spurt out from circumnuclear starburst regions, including radiation forces from a starburst as well as an AGN. The results are summarized as follows:

1. In the case in which the starburst luminosity is higher than the AGN luminosity, gas clouds are distributed at several hundred parsecs above the galactic disk as a result of the radiation pressure from the starburst. The covering factor of these clouds reaches around 20% at maximum. Accordingly, as the starburst dims, gas clouds with large optical depth are formed by cloud-cloud collisions and fall back because of the reduced radiation pressure by starburst. The larger gas clouds that have optical depth of several tens are eventually distributed near the equatorial plane. This starburst-dominant case is qualitatively consistent with the fact that Seyfert 2 galaxies appear to be more frequently associated with starbursts than Seyfert 1 galaxies.
2. In the case in which the AGN luminosity is dominant and super-Eddington, most gas clouds are blown out by the radiation pressure from the AGN. As a result, starburst-origin gas clouds hardly contribute to the obscuration of the AGN. Hence, the AGN is likely to be observed as type 1 with high probability. This AGN-dominant case corresponds to a quasar-like object. Furthermore, it is predicted that the fraction of obscured AGNs decreases with increasing AGN luminosity. This prediction matches the fraction of X-ray–absorbed AGNs found by Ueda et al. (2003).
3. The velocity dispersion of gas clouds is several 100 km s^{-1}, which is just comparable to that found in NLRs. The observations for the ionization parameter of NLRs and the extension of NLRs depending on AGN luminosity are consistent with this picture.

In this analysis, we have found that starburst-origin gas clouds can contribute to obscuration, especially on large scales. It also turns out that there is still something missing in accounting for all the properties of AGN obscuration. It may be worth considering further effects such as the combination of inner and outer obscuring materials.

We are grateful to N. Kawakatsu and K. Ohsuga for helpful discussions. We also thank the anonymous referee for valuable comments. This work was carried out with computational facilities at the Center for Computational Sciences, University of Tsukuba. M. U. acknowledges Grants-in-Aid for Scientific Research from MEXT, 16002003.

REFERENCES

Antonucci, R. 1993, ARA&A, 31, 473
Barth, A. J., Ho, L. C., Filippenko, A. V., & Sargent, W. L. W. 1995, AJ, 110, 1009
Barvainis, R., Antonucci, R., & Coleman, Paul. 1992, ApJ, 399, L19
Bassani, L., Dadina, M., Maiolino, R., Salvati, M., Risaliti, G., della Ceca, R., Matt, G., & Zamorani, G. 1999, ApJS, 121, 473
Bennert, N., Falcke, H., Schulz, H., Wilson, A. S., & Wills, B. J. 2002, ApJ, 574, L105
Blandford, R. D., Netzer, H., Woltjer, L., Courvoisier, T., & Mayor, M. 1990, Active Galactic Nuclei (Berlin: Springer)
Blandle, B., et al. 1996, ApJ, 466, 254
Brotherton, M. S., et al. 1999, ApJ, 520, L87

Buta, R., Purcell, G. B., & Crocker, D. A. 1995, AJ, 110, 1588
Canalizo, G., & Stockton, A. 2000a, ApJ, 528, 201
———. 2000b, AJ, 120, 1750
Charlot, S., Ferrari, F., Mathews, G. J., & Silk, J. 1993, ApJ, 419, L57
Dietrich, M., & Wilhelm-Erkens, U. 2000, A&A, 354, 17
Doane, J. S., & Mathews, W. G. 1993, ApJ, 419, 573
Dopita, M. A., Groves, B. A., Sutherland, R. S., Binette, L., & Cecil, G. 2002, ApJ, 572, 753
Doyon, R., Puxley, P. J., & Joseph, R. D. 1992, ApJ, 397, 117
Efstahiou, A., Rowan-Robinson, M., & Siebenmorgen, R. 2000, MNRAS, 313, 734
Elmouttie, M. Koribalski, B. Gordon, S. Taylor, K. Houghton, S. Lavezzi, T. Haynes, R., & Jones, K. 1998, MNRAS, 297, 49
Forbes, D. A., Norris, R. P., Williger, G. M., & Smith, R. C. 1994, AJ, 107, 984
Genzel, R., Weitzel, L., Tacconi-Garman, L. E., Blietz, M. Cameron, M., Krabbe, A., Lutz, D., & Sternberg, A. 1995, ApJ, 444, 129
Gonzalez Delgado, R. M., Heckman, T., & Leitherer, C. 2001, ApJ, 546, 845
Goodrich, R. W. 1995, ApJ, 440, 141
Goodrich, R. W., Veilleux, S., & Hill, G. J. 1994, ApJ, 422, 521
Hamann, F., & Ferland, G. 1993, ApJ, 418, 11
Heckman, T. M., Blitz, L., Wilson, A. S., & Armus, L. 1989, ApJ, 342, 735
Hill, J. K., Isensee, J. E., Cornett, R. H., Bohlin, R. C., O'Connell, R. W., Roberts, M. S., Smith, A. M., & Stecher, T. P. 1994, ApJ, 425, 122
Hunt, L. K., Malkan, M. A., Salvati, M., Mandolesi, N., Palazzi, E., & Wada, R. 1997, ApJS, 108, 229
Imanishi, M., & Dudley, C. C. 2000, ApJ, 545, 701
Kawakatu, N., & Umemura, M. 2004, ApJ, 601, L21
Kawakatu, N., Umemura, M., & Mori, M. 2003, ApJ, 583, 85
Lang, K. R. 1974, Astrophysical Data: Planets and Stars (Berlin: Springer)
Leitherer, C., Vacca, W. D., Conti, P. S., Filippenko, A. V., Robert, C., & Sargent, W. L. W. 1996, ApJ, 465, 717
Maiolino, R., Krabbe, A., Thatte, N., & Genzel, R. 1998a, ApJ, 493, 650
Maiolino, R., & Rieke, G. H. 1995, ApJ, 454, 95
Maiolino, R., Ruiz, M., Rieke, G. H., & Keller, L. D. 1995, ApJ, 446, 561
Maiolino, R., Ruiz, M., Rieke, G. H., & Papadopoulos, P. 1997, ApJ, 485, 552
Maiolino, R., Salvati, M., Bassani, L., Dadina, M., della Ceca, R., Matt, G., Risaliti, G., & Zamorani, G. 1998b, A&A, 338, 781
Malkan, M. A., Gorjian, V., & Tam, R. 1998, ApJS, 117, 25
Maoz, D., Barth, A. J., Sternberg, A., Filippenko, A. V., Ho, L. C., Macchetto, F. D., Rix, H. W., & Schneider, D. P. 1996, AJ, 111, 2248
Marconi, A., & Hunt, L. K. 2003, ApJ, 589, L21
Marconi, A., Moorwood, A. F. M., Origlia, L., & Oliva, E. 1994, Messenger, 78, 20
Mathis, J. S., Rumpl, W., & Nordsieck, K. H. 1977, ApJ, 217, 425
Matt, G., et al. 1996, MNRAS, 281, L69
———. 1999, A&A, 341, L39
Mauder, W., Weight, G., Appenzeller, I., & Wagner, S. J. 1994, A&A, 285, 44
McLeod, K. K., & Rieke, G. H. 1995, ApJ, 441, 96
Miller, J. S., Goodrich, R. W., & Mathews, W. G. 1991, ApJ, 378, 47
Nagasawa, M., & Miyama, S. M. 1987, Prog. Theor. Phys., 78, 1250
Norman, C. A., & Ikeuchi, S. 1989, ApJ, 345, 372
Ohsuga, K., & Umemura, M. 1999, ApJ, 521, L13
———. 2001, ApJ, 559, 157
Ohta, K., Yamada, T., Nakanishi, K., Kohno, K., Akiyama, M., & Kawabe, R. 1996, Nature, 382, 426
Oliva, E., Marconi, A., & Moorwood, A. F. M. 1999, A&A, 342, 87
Omont, A., Petitjean, P., Guilloteau, S., McMahon, R. G., Solomon, P. M., & Pecontal, E. 1996, Nature, 382, 428
Perez-Olea, D. E., & Colina, L. 1996, ApJ, 468, 191
Pogge, R. W. 1989, ApJ, 345, 730
Richstone, D., et al. 1998, Nature, 395, 14
Risaliti, G., Maiolino, R., & Salvati, M. 1999, ApJ, 522, 157
Rix, H.-W., Rieke, G., Rieke, M., & Carleton, N. P. 1990, ApJ, 363, 480
Roche, P. F., Aitken, D. K., Smith, C. H., & Ward, M. J. 1991, MNRAS, 248, 606
Rodríguez-Ardila, A., & Viegas, S. M. 2003, MNRAS, 340, L33
Rudy, R. J., Cohen, R. D., & Ake, T. B. 1988, ApJ, 332, 172
Schinnerer, E., Eckart, A., & Tacconi, L. J. 1998, ApJ, 500, 147
Schmitt, H. R. 1998, ApJ, 506, 647
Schmitt, H. R., Storchi-Bergmann, T., & Fernandes, R. C. 1999, MNRAS, 303, 173
Shapiro, P. S., & Field, G. B. 1976, ApJ, 205, 762
Solomon, P., Vanden Bout, P., Carilli, C., & Guelin, M. 2003, Nature, 426, 636
Spizer, L., Jr. 1978, Physical Processes in the Interstellar Medium (New York: Wiley)
Storchi-Bergmann, T., Raimann, D., Bica, E. L. D., & Fraquelli, H. A. 2000, ApJ, 544, 747
Storchi-Bergmann, T., Wilson, A. S., & Baldwin, J. A. 1996, ApJ, 460, 252
Tomisaka, K., & Ikeuchi, S. 1986, PASJ, 38, 697
Ueda, Y., Akiyama, M., Ohta, K., & Miyaji, T. 2003, ApJ, 598, 886
Umemura, M. 2001, ApJ, 560, L29
Umemura, M., Fukue, J., & Mineshige, S. 1997, ApJ, 479, L97
———. 1998, MNRAS, 299, 1123
Wada, K., & Norman, C. A. 2002, ApJ, 566, L21
Wilson, A. S., Helfer, T. T. Haniff, C. A., & Ward, M. J. 1991, ApJ, 381, 79